

## Measurements of eddy correlation oxygen fluxes in shallow freshwaters: Towards routine applications and analysis

Daniel F. McGinnis,<sup>1</sup> Peter Berg,<sup>2</sup> Andreas Brand,<sup>1,3</sup> Claudia Lorrai,<sup>1,3</sup> Theresa J. Edmonds,<sup>1</sup> and Alfred Wüest<sup>1,3</sup>

Received 27 November 2007; revised 4 January 2008; accepted 14 January 2008; published 16 February 2008.

[1] Benthic fluxes of dissolved oxygen are measured in a shallow reservoir using the eddy correlation technique. Flux variations depict the diurnal production-consumption cycle, with daytime oxygen release following the solar radiation trend. The average nighttime uptake of  $-40 \pm 11 \text{ mmol m}^{-2} \text{ d}^{-1}$  is in excellent agreement with the rate of  $-35 \pm 3 \text{ mmol m}^{-2} \text{ d}^{-1}$  derived from sediment oxygen micropores. Separating large-scale advective and turbulent fluctuations is a crucial and uncertain component of the flux computation and the largest source of error. To compensate for the 2.25 s oxygen sensor response time, the oxygen flux calculations are corrected by only  $\sim 5\%$  using a first-order spectral enhancement. This work demonstrates that only a slightly faster oxygen sensor would be needed to resolve the entire flux spectrum. The 18 hours of data are the first measurements obtained in a freshwater reservoir that capture the diurnal oxygen production-consumption cycle. **Citation:** McGinnis, D. F., P. Berg, A. Brand, C. Lorrai, T. J. Edmonds, and A. Wüest (2008), Measurements of eddy correlation oxygen fluxes in shallow freshwaters: Towards routine applications and analysis, *Geophys. Res. Lett.*, 35, L04403, doi:10.1029/2007GL032747.

### 1. Introduction and Eddy Correlation Technique

[2] In lakes and reservoirs, a prime question concerns the flux of dissolved oxygen (DO) through the sediment-water interface. In this study, DO fluxes 15 cm above the sediment are directly measured using the eddy correlation (EC) technique. While this method has been previously implemented for measuring constituent fluxes in the atmosphere [Lee *et al.*, 2004] and heat fluxes in the ocean [Shirasawa *et al.*, 1997], the application of the EC technique for measuring DO fluxes in stratified waters is novel, with only four measurement studies reported so far; three from marine systems [Berg *et al.*, 2003, 2007; Kuwae *et al.*, 2006] and one from a freshwater lake (A. Brand *et al.*, Intermittency of oxygen flux into the bottom boundary of lakes as observed by eddy correlation, submitted to *Limnology and Oceanography*, 2008).

[3] The EC technique has several distinct advantages over traditional DO uptake measurement methods (e.g. in situ chambers, DO sediment micropores) [Berg *et al.*,

2003]. The most obvious advantage is that the EC technique does not disturb the sediment and natural hydrodynamics. Another important advantage lies in the temporal resolution, as we now have the possibility to measure fluxes continuously on the time scale of minutes.

[4] The EC instrumentation consists of a DO sensor deployed simultaneously with an acoustic Doppler velocimeter (Figure 1, left) as first proposed and implemented by Berg *et al.* [2003, 2007]. We applied the technique in a shallow, run-of-river reservoir (Lake Wohlen, Switzerland). To our knowledge, the 18 hours of data presented here are the first such measurement obtained in freshwater that captures the diurnal benthic oxygen production-consumption cycle. Given the obvious benefits of the EC technique, we ultimately strive for an easily deployable EC instrument combined with routine protocol for data analysis.

[5] Below, we first describe the EC instrumentation, then the data processing and spectral DO response-time corrections (section 2). The subsequent presentation of the application to the run-of-river reservoir and resulting flux estimates (section 3) include a discussion of analysis requirements and appropriate data treatment. Finally, we show that our 2.25 s DO sensor response results in only a 5% loss of the DO flux estimates.

### 2. Methods

[6] The DO flux is expressed as  $w\text{DO}$ , where  $w$  (vertical velocity) and DO (concentration) can be broken down into the mean and fluctuating components,  $\bar{w} + w'$  and  $\bar{\text{DO}} + \text{DO}'$  [Reynolds, 1895; Berg *et al.*, 2003]. For DO fluxes towards the sediment, the typical DO fluctuation ( $\text{DO}'$ ) is higher than the mean when the vertical velocity fluctuation ( $w'$ ) points towards the sediment and vice versa (see Figure 1, middle).

#### 2.1. Eddy Correlation Device

[7] The EC device consists of a velocimeter (Vector, Nortek, www.nortek-as.com) and a Clark-type oxygen micro-electrode from Unisense (www.unisense.com; 90% response time  $< 0.3 \text{ s}$ ) that allow simultaneous measurements of near-sediment velocity and DO concentrations (Figure 1, middle). The electronics amplifying the microelectrode signal consist of a precision pico-amplifier in series with a guard circuit. A sampling volume location device (c in Figure 1, left) is used to position the DO sensor tip (b) close to the velocimeter measurement volume and is removed before deployment.

#### 2.2. Data Analysis

##### 2.2.1. Time Corrections

[8] The main factor affecting the DO response time is the amplifier response ( $\sim 2 \text{ s}$ ), and to a much lesser extent, the

<sup>1</sup>Surface Waters - Research and Management, Eawag, Kastanienbaum, Switzerland.

<sup>2</sup>Department of Environmental Sciences, University of Virginia, Charlottesville, Virginia, USA.

<sup>3</sup>Institute of Biogeochemistry and Pollutant Dynamics, ETH Zurich, Zurich, Switzerland.

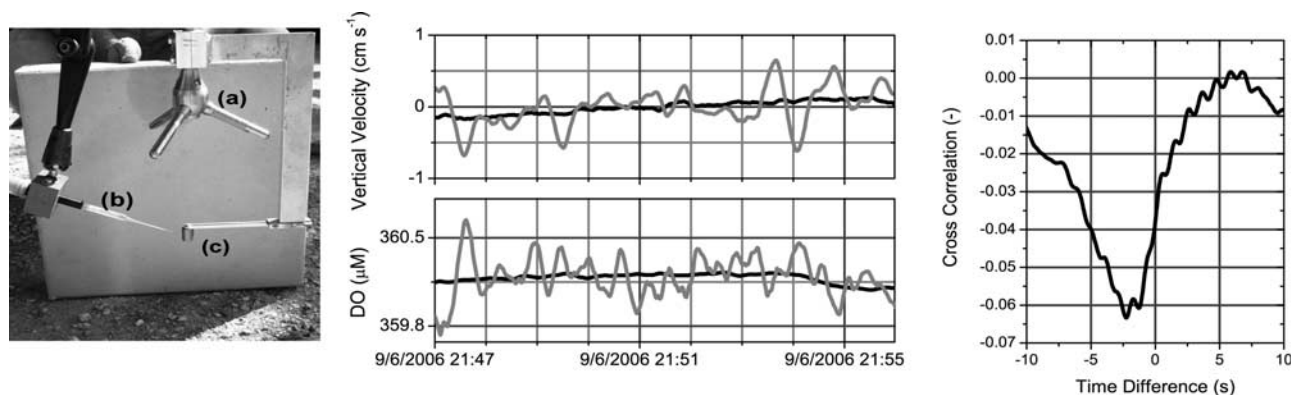


**Figure 1.** (left) Eddy correlation instrument. Three-beam Nortek Vector (a) with Unisense dissolved oxygen (DO) sensor (b) and artificial measurement volume for positioning the DO sensor (removed during deployment) (c). (middle) Nine minutes data collected at Lake Wohlen: (top) vertical velocity and (bottom) DO. Black lines indicate running averages, grey lines are data (smoothed for clarity). (right) Cross correlation as a function of shifting DO time series ahead the velocity data series. The maximum negative correlation is  $\sim 2.25$  s.

travel time (lag) between the DO sensor tip and velocity sampling volume (distance is  $\sim 1$  cm). Because the DO signal reacts slower than the velocimeter, the DO data series are shifted back in time relative to the velocity series (Figure 1, right) until the maximum flux (correlation) is obtained. To verify this approach, the cross correlation is calculated to obtain the maximum (negative for consumption, positive for production) correlation between DO and velocity (Figure 1, right). Both procedures suggest an  $\sim 2.25$  s time correction.

[9] The DO spectra and calculated cospectra of  $w'$  and  $DO'$  are then corrected for the frequency-dependent damping [Eugster and Senn, 1995; Gregg, 1999]. Basically, high-frequency DO spectral contributions are “enhanced” to correct for that part of the signal that is lost due to response times. For linear damping, the correction function is

$$S_{DO,corr}(f) = (1 + f^2\tau^2)S_{DO,meas}$$

where  $S_{DO,corr}$  ( $\mu M^2 s$ ) is the DO power spectrum corrected for response time  $\tau$  (s) from the measured  $S_{DO,meas}$ , and  $f$  is frequency (Hz). The cospectra are enhanced by the same procedure. By integrating the enhanced cospectra, we determined that  $<5\%$  of the flux signal is lost due to the finite DO sensor response time (Figure 2, left).

### 2.2.2. Eddy Flux Calculations

[10] The DO fluxes are calculated from raw velocity and DO data using the software package EddyFlux Version 1.3 beta. It uses three independent methods to remove the means from raw data (mean removal, linear detrending, and filtering by running averaging; see for example Lee *et al.* [2004]) to extract  $w'$  and  $DO'$ .

### 2.2.3. Sediment Flux Calculations

[11] Flux estimates were obtained from DO microprofiles (Figure 2, right) measured in the top few mm of the sediment by a simultaneously deployed lander [Müller *et al.*, 2002]. The vertically well-resolved profiles allow the DO flux to be calculated at the sediment-water interface from the concentration-depth profile [Berg *et al.*, 1998] and from the vertically integrated DO depletion rate [see Müller *et al.*, 2002].

## 2.3. Study Site and Campaign

[12] The study was conducted at Lake Wohlen, a run-of-river reservoir located on the Aare River (Bern, Switzerland). Lake Wohlen has a surface area of  $3.65 \text{ km}^2$  and a maximum depth of 20 m. From 5 to 7 September 2006, EC measurements were performed in  $\sim 3$  m water depth, 15 cm above the sediment with a sampling rate of 32 Hz. The EC device was deployed on a rigid aluminum tripod with two legs orthogonal to the main flow direction and the third leg downstream from the sensors. Our two deployments spanned an  $\sim 38$ -hr time range: deployment 1 from 5 Sept 14:00 to 6 Sept 06:00 and deployment 2 from 6 Sept 09:30 to 7 Sept 02:00, 2006 (CEST). The oxygen sensor was calibrated in the laboratory before and after the deployment and showed negligible drift.

## 3. Results and Discussion

[13] In this section, we firstly present the eddy flux results. Next, we discuss the determination of the running average window size. We then analyze the spectral contri-

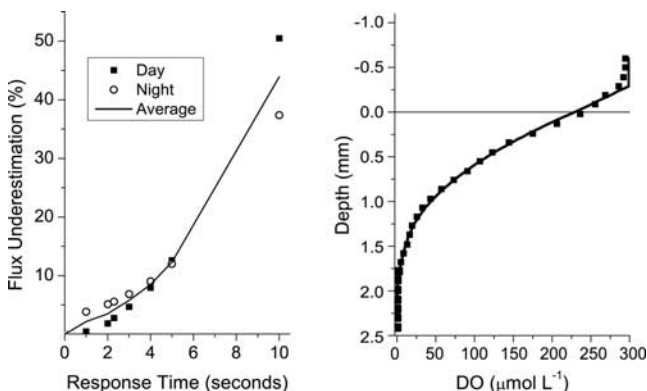


**Figure 2.** (left) Flux correction in % enhancement as a function of the DO sensor/amplifier response time. (right) DO microprofile obtained from lander deployment in the top 2.5 mm of the sediment near eddy correlation device.

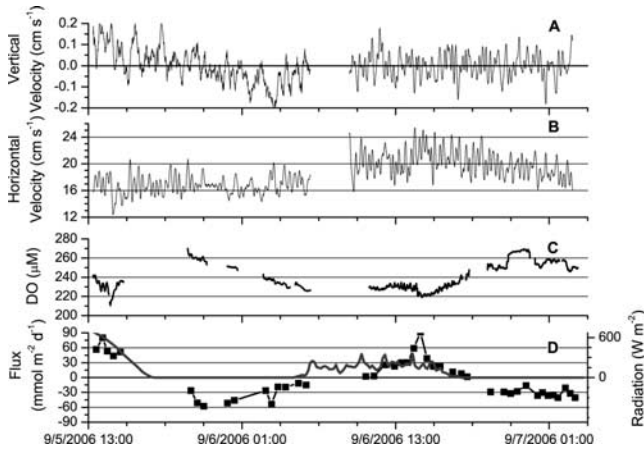


**Figure 3.** Eddy correlation data and flux calculations (5 to 7 Sep 2006). (a) Vertical and (b) horizontal velocity (gap is when instrument was removed, downloaded, and redeployed). (c) DO values (additional data gaps are due to corrupt DO data – see text). (d) Calculated fluxes (black) and solar radiation (grey).

bution of the eddies. Using the DO spectra, we illustrate that there is no clear spectral gap between large-scale advective fluxes and the smaller scale turbulent fluxes, emphasizing the importance of appropriate mean removal to determine the fluctuations. Finally, we address DO response time compensation.

### 3.1. Overview of Flux Estimates

[14] Figures 3a, 3b, and 3c show the measured horizontal velocity, vertical velocity and DO values used for the flux estimates. Figure 3d gives individual fluxes calculated from  $\sim 0.25$  to 1 hr time intervals (depending on quality of time

series). The dark-grey line on Figure 3d (right-axis) shows the global radiation (data: MeteoSwiss). Parts of the time series were omitted from the analysis shown on Figure 3d due to corrupted data, probably caused by floating debris or electrical interference.

[15] The DO fluxes convincingly demonstrate the effect of photosynthesis on the benthic DO exchange. The fluxes are high during the day, with peak releases of  $54 \pm 13$  (SD)  $\text{mmol m}^{-2} \text{d}^{-1}$  on 5 Sept (clear sky) and  $36 \pm 22$  (SD)  $\text{mmol m}^{-2} \text{d}^{-1}$  on 6 Sept (cloudy sky), following the trend in global solar radiation. Nighttime DO uptake varies from  $-47 \pm 14$  (SD)  $\text{mmol m}^{-2} \text{d}^{-1}$  during the first night, to  $-34 \pm 6$  (SD)  $\text{mmol m}^{-2} \text{d}^{-1}$  during the second night (measurement locations were about 3 meters apart), with the overall average nighttime flux for both nights of  $-40 \pm 11$  (SD)  $\text{mmol m}^{-2} \text{d}^{-1}$ . This value is in very good agreement with the  $-35 \pm 3$  (SD)  $\text{mmol m}^{-2} \text{d}^{-1}$  estimated from the nearby lander DO microprofiles (Figure 2, right).

### 3.2. Sensitivity of Spectral Flux Contributions

[16] When extracting the fluctuations using running mean, it is an intrinsic difficulty to determine the appropriate averaging window length. The number of data points used must be long enough to encompass all of the flux contributing eddy sizes, but not too long as to include artifacts such as sensor drift or non-turbulent (reversible) changes. Figure 4 (left) illustrates the sensitivity of the flux estimations as a function of averaging window size. The averaging window analysis is initiated with a flux calculation based on a narrow window for the running averages (1 data point gives a flux of zero on Figure 4 (left) and proceeds from right to left along horizontal axis as averaging window size increases). The averaging window is expanded step-wise and the flux is recalculated. By increasing the averaging window size and repeating the flux calculation, the outcome is basically the cumulative addition

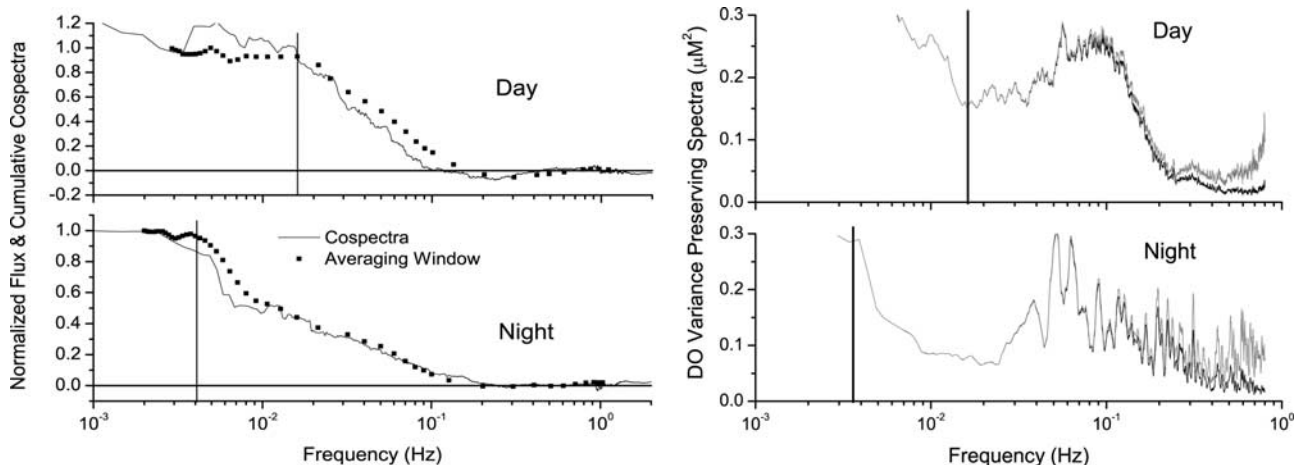


**Figure 4.** (left) Normalized DO fluxes for  $\sim 30$ -min long time series (points) during day- and nighttime, as estimated for different lengths of the averaging window. These DO fluxes compare well to those calculated from the cumulative cospectra (solid line). Vertical lines represent estimates of low frequency cutoffs for turbulent contributions. Figure is read from right- to left-side along x-axis. (right) Variance-preserving DO spectrum (frequency  $\times$  spectral density ( $S_{DO}$ )) for entire day- and nighttime data series. The grey curve represents the variance-preserving spectra corrected for response time of DO sensor. Basin-scale waves (both surface and internal) have a frequency of  $\sim 5 \times 10^{-4}$  to  $5 \times 10^{-3}$  Hz ( $\sim 3$  to 33 minutes) in Lake Wohlen.



of the value of the spectral contributions. For comparison, the cumulative cospectra of  $w'$  and  $DO'$  are calculated. As shown in Figure 4 (left), the calculated cumulative cospectra yield the same flux as the averaging window-size analysis.

[17] The results of the two described analyses indicate that both methods can be used to determine the frequency cutoffs for the eddy spectral contributions. As shown on Figure 4 (left), fluxes reach nearly their maxima at  $\sim 17 \times 10^{-3}$  Hz ( $\sim 60$  s) during the day and  $\sim 4 \times 10^{-3}$  Hz ( $\sim 250$  s) at night, before they level off (indicated by solid vertical lines in Figure 4). At the other end of the spectrum, the maximum frequency of eddies contributing to the flux appears to be at 0.2 to 0.3 Hz ( $\sim 3$  to 5 s; point at which curve begins to diverge from horizontal) for both methods and does not vary significantly between daytime and nighttime.

[18] In the so-called “variance-preserving” plot of the DO spectrum (frequency  $\times S_{DO}$ , where  $S_{DO}$  is the DO power spectrum), the area under the curve is proportional to the contribution of the total DO variance [Gregg, 1999]. The variance-preserving plots on Figure 4 (right) indicate from which spectral range most of the DO contributions are to be expected for both the daytime and nighttime data (grey line shows corrected spectra). The solid vertical lines correspond with the minimum frequency of spectral contributions shown in Figure 4 (left). At the lower frequencies ( $< 1 \times 10^{-2}$  Hz), the effects of basin-scale waves (both surface and internal seiche) can be seen, which have a frequency around  $\sim 5 \times 10^{-4}$  to  $5 \times 10^{-3}$  Hz ( $\sim 3$  to 33 minutes) in Lake Wohlen (from thermistor data, not shown).

[19] From Figure 4, it is not always clear where to place the low frequency cutoff when defining the averaging window, as there is no obvious spectral gap between the large scale, advective contributions, and smaller-scale eddies. This is particularly visible from the daytime variance-preserving spectral plot. We view this as the biggest challenge in eddy correlation flux extractions and therefore conclude that the largest uncertainties associated with the technique are rooted here.

### 3.3. Time Scales

[20] The eddy time scales contributing to the signal range from  $\sim 3$  to 60 s during the day and from  $\sim 3$  to 250 s at night. During the day, Lake Wohlen may slightly stratify and suppress larger eddies. However, at night the water column is completely well-mixed, resulting in the maximum eddy size being limited only by the depth of the water.

[21] For comparison, the smallest expected eddy size can be estimated by the Kolmogorov length scale,  $L_K = (\nu^3/\varepsilon)^{1/4}$ . Using a kinematic viscosity of  $\nu = 1.5 \times 10^{-6}$  m<sup>2</sup> s<sup>-1</sup> and a turbulent dissipation estimate of  $\varepsilon = 1 \times 10^{-7}$  W kg<sup>-1</sup> yields minimum eddy sizes  $L_K$  in the range of  $\sim 2$  mm with a minimum time scale  $(L_K^2/\varepsilon)^{1/3}$  of  $\sim 4$  s [Wüest and Lorke, 2003].

### 3.4. Noise

[22] Figure 4 (right) indicates peaks at around 1 Hz for DO. Higher frequency noise is present in both the velocity and DO data. It is suspected that this noise may be caused by the  $\sim 1$  Hz internal compass readings (ENU coordinates), which will be disabled during future measurements. How-

ever, as expected, the noise of  $w$  and DO are uncorrelated and do not significantly contribute to the fluxes.

## 4. Summary

[23] The eddy correlation dissolved oxygen (DO) fluxes ( $-40 \pm 11$  mmol m<sup>-2</sup> d<sup>-1</sup>) compare well with the lander microprofile DO fluxes ( $-35 \pm 3$  mmol m<sup>-2</sup> d<sup>-1</sup>). To determine the most accurate eddy correlation fluxes, it was necessary to account for the DO response time by both (1) shifting the DO data back in time, and (2) enhancing the damped spectral contributions due to the  $\sim 2$  s response time of our amplifier by a first order linear correction. We found that shifting the DO time series 2.25 s backwards maximized the fluxes, and that only a slightly faster sensor would be needed to obtain the entire signal. However, the entire signal can also be closely estimated by enhancing the spectra numerically.

[24] Selection of the appropriate time-averaging window for the running mean must be done to ensure that all of the turbulent flux contributions are included, and all reversible (e.g. basin scale internal waves) motions are excluded. However, the absence of distinct spectral gaps makes this task more uncertain, and leads to some overlap (and hence uncertainties) from these two categories of contributions. For the data presented here, we estimate that the spectral-gap uncertainties potentially cause the largest errors in flux estimates, possibly up to 10% based on sensitivity analyses and how well the spectral gap can be resolved. We have further shown that even for the same locations, the length of the averaging window can substantially vary between day- and nighttime. The different averaging time scales are associated with changing spectral contributions related to the water column stability (i.e. larger eddies are suppressed during daytime stratification).

[25] Overall, the results show that the eddy correlation technique is a promising method for determining DO fluxes in natural water bodies. With this unique data set collected over  $\sim 38$ -hr, we were able to demonstrate the diurnal benthic DO production-consumption cycle. The DO production fluxes relate well with the nearby measured solar radiation while nighttime consumption was relatively constant and agrees with results obtained from DO sediment microprofiles. With the eddy correlation technique, we are now able to resolve the high temporal variability (minutes) of the sediment DO fluxes, which until now could only be resolved on the time scale of hours to days using traditional measurement techniques. Furthermore, the measurement and analysis of eddy correlation data have the added advantage of resolving many bottom-boundary layer hydrodynamic properties.

[26] The eddy correlation technique is limited to constituents that can be measured with relatively fast sensors. However, in this work we have demonstrated that sensors with response times of (several) seconds could potentially be used. Currently, instrument deployment lengths are limited to internal memory and battery capacities, and DO sensor fouling considerations.

[27] Taken together, the analysis described here allows a controlled and consistent protocol to estimate the DO flux, spectral contributions and potential errors. The procedure is still in the early stages of application in aquatic systems, and

many more data must be collected and analyzed to reveal the full capability of this new technique.

[28] **Acknowledgments.** We would like to express our gratitude to C. Dinkel, D. Richter, and M. Schurter for assisting in the development and testing of the equipment. Additional thanks to the anonymous reviewers and W. Eugster for their valuable suggestions. The study was supported by the Swiss National Science Foundation (grants 200020-103827.1 and 200020-111763.1) and Eawag.

## References

- Berg, P., N. Risgaard-Petersen, and S. Rysgaard (1998), Interpretation of measured concentration profiles in sediment pore water, *Limnol. Oceanogr.*, **43**(7), 1500–1510.
- Berg, P., H. Røy, F. Janssen, V. Meyer, B. B. Jørgensen, M. Huettel, and D. de Beer (2003), Oxygen uptake by aquatic sediments measured with a novel non-invasive eddy-correlation technique, *Mar. Ecol. Prog. Ser.*, **261**, 75–83.
- Berg, P., H. Røy, and P. L. Wiberg (2007), Eddy correlation flux measurements: The sediment surface area that contributes to the flux, *Limnol. Oceanogr.*, **52**(4), 1672–1684.
- Brand, A., D. F. McGinnis, B. Wehrli, and A. Wüest (2008), Intermittency of oxygen flux into the bottom boundary of lakes as observed by eddy correlation, *Limnol. Oceanogr.*, in press.
- Eugster, W., and W. Senn (1995), A cospectral correction model for measurement of turbulent NO<sub>2</sub> flux, *Boundary Layer Meteorol.*, **74**(4), 321–340.
- Gregg, M. C. (1999), Uncertainties and limitation in measuring  $\varepsilon$  and  $\chi_T$ , *J. Atmos. Oceanic Technol.*, **16**(11), 1483–1490.
- Kuwae, T., K. Kamio, T. Inoue, E. Miyoshi, and Y. Uchiyama (2006), Oxygen exchange flux between sediment and water in an intertidal sand-flat, measured in situ by the eddy-correlation method, *Mar. Ecol. Prog. Ser.*, **307**, 59–68.
- Lee, X., W. Massman, and B. Law (Eds.) (2004), *Handbook of Micrometeorology: A Guide for Surface Flux Measurement and Analysis*, 250 pp., Kluwer Acad., Dordrecht, Netherlands.
- Müller, B., M. Mäerki, C. Dinkel, R. Stierli, and B. Wehrli (2002), In situ measurements in lake sediments using ion-selective electrodes with a profiling lander system, in *Environmental Electrochemistry: Analysis of Trace Element Biogeochemistry*, edited by M. Taillefert and T. F. Rozan, pp. 126–143, *ACS Symp. Ser.*, vol. 811, Am. Chem. Soc., Washington, D. C.
- Reynolds, O. (1895), On the dynamical theory of incompressible viscous fluids and the determination of the criterion, *Philos. Trans. R. Soc. London, Ser. A.*, **186**, 123–164.
- Shirasawa, K., R. G. Ingram, and E. J. J. Hudier (1997), Oceanic heat fluxes under thin sea ice in Saroma-ko Lagoon, Hokkaido, Japan, *J. Mar. Syst.*, **11**(1–2), 9–19.
- Wüest, A., and A. Lorke (2003), Small-scale hydrodynamics in lakes, *Annu. Rev. Fluid Mech.*, **35**, 373–412.

P. Berg, Department of Environmental Sciences, University of Virginia, Charlottesville, VA 22904-4123, USA.

A. Brand, T. J. Edmonds, C. Lorrai, D. F. McGinnis, and A. Wüest, Surface Waters - Research and Management, Eawag, Seestrasse 79, CH-6047 Kastanienbaum, Switzerland. (dan.mcginnis@eawag.ch)